

OBSERVATION OF ELECTRONIC SHELLS IN LARGE LITHIUM CLUSTERS

C.BRECHIGNAC, Ph.CAHUZAC, M.de FRUTOS, J.Ph.ROUX and
K.BOWEN*
Laboratoire Aimé Cotton
CNRS II bât. 505
91405 Orsay cedex, France

ABSTRACT. Shell and supershell structures have been observed for lithium clusters produced in a gas-aggregation type source, up to the size range $n \lesssim 2000$. Noteworthy similarities are found as compared with observations performed on Na_n clusters. Thermal effects are briefly investigated.

1. INTRODUCTION.

Recent experimental efforts to extend the study of clusters to large sizes have led to the observation of electronic shells in large Na-atom clusters [1-3]. Sequences of "magic numbers" have been detected for particles containing up to 2700 atoms, from the observation of abundances in mass spectra. Extending the ideas originally proposed by Balian and Bloch [4], recent calculations show that such a shell structure must be attributed to the electronic subshells of delocalized valence electrons moving in a central potential [5,6]. The shell periodicity is proportional to the cube root of the number n of valence electrons. Superimposed to this primary shell periodicity, a beat pattern is observed. The corresponding supershell structure is explained in terms of interference of amplitude associated with classical closed orbits of electrons. The beat mode has a minimum found around 1100 valence electrons by Bjørnholm et al. [7], whereas Martin et al. determined the transient region around $n=830$ [3,8]. Calculations are able to reproduce both values, depending on the detailed shape of the radial potential [3,5,6]. We present here new results obtained on lithium clusters. We observed a shell structure up to $n=2100$ with a beat mode minimum located near $n=900$. The temperature dependence upon the observability of the shell structure is also investigated.

2. EXPERIMENT.

The Li clusters are produced by a gas-aggregation type source [3,9-11]. The metal vapor is produced at a moderate pressure, a few of 0.1 torr, by heating a molybdenum oven. Metal atoms effuse in a helium flow through a 4 mm hole (Fig.1). They are carried along by 20-25 torr of helium into a 6cm long, liquid nitrogen cooled copper tube. The metal clusters grow along the helium stream which progressively cools them and dissipates their formation energy. The cluster growth stops at the end of the tube, where the metal cluster-helium mixture enters the three successive chambers of a differential pumping system.

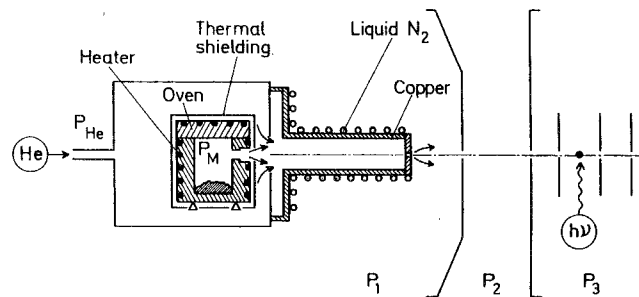


Figure 1 : Schematic of our gas-aggregation source. For 20 torr of He, the differential pressures $P_{1,2,3}$ are typically 0.5 torr, 210^{-4} and 510^{-6} torr respectively. The hole diameter in the liquid nitrogen cooled copper tube is 2mm.

The neutral particles are photoionized at a photon energy $h\nu=3.50$ eV provided by the third harmonic of a pulsed Nd-YAG laser. Ionization takes place in between a multiplate accelerating system of a Wiley-Mc Laren time-of-flight mass spectrometer [12]. The length of the drift tube is 120cm and typically Li_n clusters are accelerated to 2.8 kV. A secondary electron multiplier delivers ion signals averaged by a Le Croy 9400 digital oscilloscope. With this source a pseudo-gaussian distribution of neutral Li_n clusters is generated, the mean size of which is quite sensitive to the metal vapor pressure. Varying this latter from 510^{-2} torr to 510^{-1} torr, promotes a shift of the maximum from $n=200$ to $n=900$. Simultaneously the relative width $\Delta n/n$ is increasing from 0.6 to 1.2 respectively. Such a source gives medium-size clusters [11]. This differs from those obtained by other gas-aggregation sources which generate only large neutral clusters [3,10].

RESULTS.

At low laser fluence (1 mW/cm^2) one observes s-shaped irregularities superimposed on the envelope of the size distribution (Fig.2). When the metallic vapor pressure is varied, the envelope shifts, whereas these structures remain fixed in time, and so in size. They appear with a modulation which decreases at large size, beyond the maximum of the distribution. These features must be attributed to electronic shells of the valence electrons as observed by other authors with Na_n clusters [2,3]. The photon energy $h\nu=3.50\text{eV}$ is chosen above the ionization potentials of large lithium clusters and in the expected range of the maximum

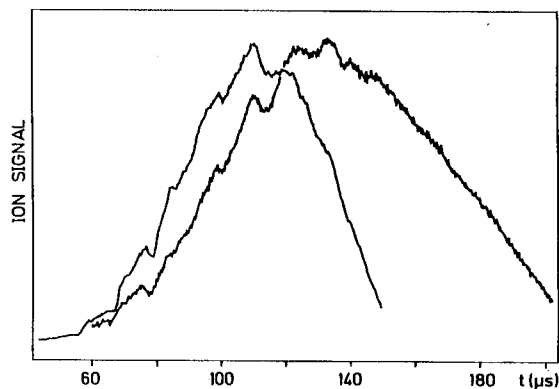


Figure 2 : Shift of the mass distribution vs the metallic vapor. Left curve : Lithium pressure 0.2 torr. Right curve : lithium pressure 0.7 torr. Successive shells are clearly visible as strong irregularities.

of the photo-absorption cross-section, so that the shells are revealed from evaporative cooling as shown in ref. [13,14]. When the laser fluence is slightly increased (up to 5 mW/cm^2), the irregularities are washed-out and a smooth profile is observed (Fig.3). Under these conditions, several photons are absorbed during the ionizing laser pulse. The subsequent dissociation shifts noticeably the mean size of the mass distribution toward smaller sizes. Indeed, each ion parent gives rise to a broad distribution of fragments [13] and the sharp structures are erased. When the laser fluence is still increased (up to few W/cm^2), the efficient multistep photoexcitation-dissociation process generates small clusters up to the monomer (Fig.4). In this case the well known shell closing effects [15] are clearly visible as an abrupt change in ion intensities after $n=3,9,21,41,69$ and 93. Mass spectra as shown on Fig.4 provide an accurate and absolute scaling of the time-of-flight mass spectrometer. However care must be taken to the use of natural lithium which contains two isotopes ${}^7\text{Li}$ (92.6%) and ${}^6\text{Li}$ (7.4%). A cluster of a given size n results on a binomial distribution of the isotopic mixture ${}^6\text{Li}_x {}^7\text{Li}_{n-x}$ with the probability $C_n^x \alpha^x (1-\alpha)^{n-x}$ [16]. C_n^x is the binomial coefficient and α is the natural abundance of the ${}^6\text{Li}$ isotope. In the limit of large n , the isotopic distribution

of the photo-absorption cross-section, so that the shells are revealed from evaporative cooling as shown in ref. [13,14]. When the laser fluence is slightly increased (up to 5 mW/cm^2), the irregularities are washed-out and a smooth profile is observed (Fig.3). Under these conditions, several photons are absorbed during the ionizing laser pulse. The subsequent dissociation shifts noticeably the mean size of the mass distribution toward smaller sizes. Indeed, each ion parent gives rise to a broad distribution of fragments [13] and the sharp structures are erased. When the laser fluence is still increased (up to few W/cm^2), the efficient multistep photoexcitation-dissociation process generates small clusters up to the monomer (Fig.4). In this case the well known shell closing effects [15] are clearly visible as an abrupt change in ion intensities after $n=3,9,21,41,69$ and 93. Mass spectra as shown on Fig.4 provide an accurate and absolute scaling of the time-of-flight mass spectrometer. However care must be taken to the use of natural lithium which contains two isotopes ${}^7\text{Li}$ (92.6%) and ${}^6\text{Li}$ (7.4%). A cluster of a given size n results on a binomial distribution of the isotopic mixture ${}^6\text{Li}_x {}^7\text{Li}_{n-x}$ with the probability $C_n^x \alpha^x (1-\alpha)^{n-x}$ [16]. C_n^x is the binomial coefficient and α is the natural abundance of the ${}^6\text{Li}$ isotope. In the limit of large n , the isotopic distribution

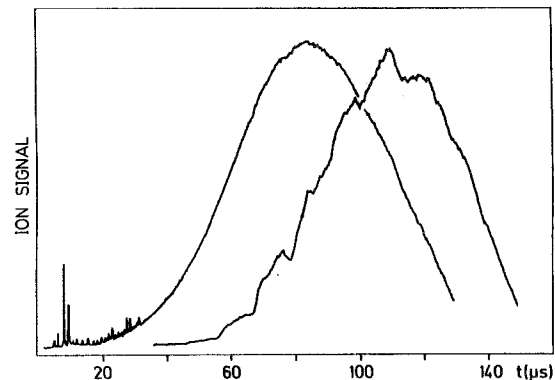


Figure 3 : Shift of the mass distribution vs the laser fluence. The profile peaked at large size is the same as Fig.2 (low metallic vapor pressure). The smooth profile shifted toward smaller time-of-flight is taken at the same lithium pressure but at a slightly higher laser fluence. Notice the occurrence of mass resolved very small size fragments.

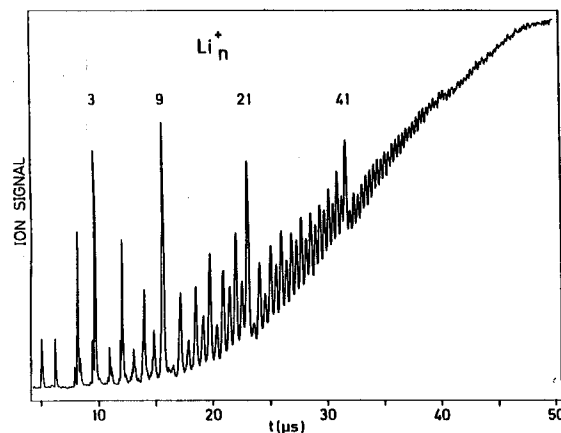


Figure 4 : Small size lithium clusters obtained by photoevaporation from large sizes. Closed shell, odd-even alternations [15] are visible. The first ion peak is due to ionized helium atoms. The rising background corresponds to the residual envelope observed at low laser fluence.

of the photo-absorption cross-section, so that the shells are revealed from evaporative cooling as shown in ref. [13,14]. When the laser fluence is slightly increased (up to 5 mW/cm^2), the irregularities are washed-out and a smooth profile is observed (Fig.3). Under these conditions, several photons are absorbed during the ionizing laser pulse. The subsequent dissociation shifts noticeably the mean size of the mass distribution toward smaller sizes. Indeed, each ion parent gives rise to a broad distribution of fragments [13] and the sharp structures are erased. When the laser fluence is still increased (up to few W/cm^2), the efficient multistep photoexcitation-dissociation process generates small clusters up to the monomer (Fig.4). In this case the well known shell closing effects [15] are clearly visible as an abrupt change in ion intensities after $n=3,9,21,41,69$ and 93. Mass spectra as shown on Fig.4 provide an accurate and absolute scaling of the time-of-flight mass spectrometer. However care must be taken to the use of natural lithium which contains two isotopes ${}^7\text{Li}$ (92.6%) and ${}^6\text{Li}$ (7.4%). A cluster of a given size n results on a binomial distribution of the isotopic mixture ${}^6\text{Li}_x {}^7\text{Li}_{n-x}$ with the probability $C_n^x \alpha^x (1-\alpha)^{n-x}$ [16]. C_n^x is the binomial coefficient and α is the natural abundance of the ${}^6\text{Li}$ isotope. In the limit of large n , the isotopic distribution

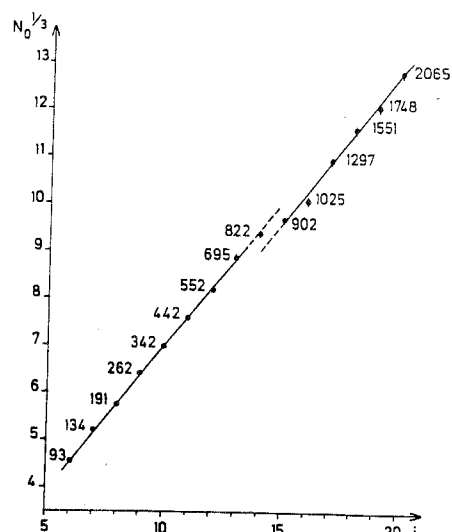


Figure 5 : Magic numbers $N_0^{1/3}$ vs the shell index and the corresponding number of valence electrons. Notice the abrupt phase-shift in the $n=800-900$ size domain

It is interesting to compare the slope of this straight line which should be independent of the nature of alkali-atoms in the cluster. We found $\Delta(N_0^{1/3})=(0.63\pm 0.03)\Delta i$, a value in excellent agreement with the value found for sodium clusters [7,8]. The absolute values found for the N_0 numbers show noteworthy similarities with those either deduced from sodium experiments [3,7,8] or calculated by using a Wood-Saxon potential or a "wine-bottle" type potential [3,5,6]. However some differences exist. Mainly we found an extremum at $n=308\pm 5$, not shown in the plot of the Fig.5. This shell is neither observed with Na_n clusters nor predicted by calculations. Keeping in mind the sensitivity of the subshell bunching to the detailed shape of the radial potential, this suggests that the potential to be considered for lithium clusters could be somewhat different with regard to the potential used for sodium clusters. Moreover, the geometrical arrangement of atoms in the clusters, can play a role in determining the magic numbers [17,18] and this cannot be totally ruled out.

CONCLUSION

This first study of shell effects in lithium clusters allows a comparison with results obtained with sodium clusters. Experimental values support the semi-classical interpretation of the shell and supershell structures. However the detailed analysis of the observations suggests the need to reconsider more accurately the radial potential shape of lithium clusters. This could be obtained from more precise measurements on isotopically enriched 7Li .

given by $\frac{\Delta n}{n} = \alpha(1 - \frac{6}{7}) = 0.01$. The

determination of the relative maxima of the shell structure is obtained by using such a corrected size calibration.

The valence electron number corresponding to the successive relative maxima as seen on Fig.2 and 3, and averaged over several mass spectra, are easily determined. In a semiclassical picture one expects a periodicity of shells proportionnal to the linear dimension of the droplet $\approx n^{1/3}$. Plotting the "magic numbers" N_0 , i.e the shell maxima, on a $n^{1/3}$ scale against a running index i , accounting for the shell number, one obtains two series of points at approximately equal intervals (Fig.5). The two straight lines are shifted relative to each other by one-half unit of i around $n\approx 900$ as found in one of the experiments performed with Na_n clusters [8]. This characterizes the beat mode minimum of a supershell structure.

ACKNOWLEDGEMENTS.

The authors would like to thank T.P.Martin for valuable and stimulating discussions.

*Permanent address : Department of Chemistry, The Johns Hopkins University, Baltimore, Maryland 21218, USA.

K.B. wishes to acknowledge the partial support of the U.S. National Science Foundation under grant CHE-9007445.

REFERENCES.

- [1] Göhlich.H, Lange.T, Bergmann.T, Martin.T.P., Electronic shell structure in large metallic clusters, *Phys. Rev. Lett.* **65**, 748-751 (1990).
- [2] Bjørnholm.S, Borggreen.J, Echt.O, Hansen.K, Pederson.J, Rasmussen.H.D., observation of electronic shells and shells of atoms in large Na clusters. *Phys. Rev. Lett.* **65**, 1627-1630 (1990).
- [3] Martin.T.P, Bergmann.T, Göhlich.H, Lange.T. Mean field quantization of several hundred electrons in sodium metal clusters. *Chem. Phys. Lett.* **176**, 343-347 (1991).
- [4] Balian.R, Bloch.C. Distribution of eigenfrequencies for the wave equation in a finite domain : III Eigenfrequency density oscillations. *Ann. Phys.* **69**, 76-160 (1972).
- [5] Nishioka.H, Hansen.K, Mottelson.B.R. Supershells in metal clusters. *Phys. Rev. B* **42**, 9377-9386 (1990-II).
- [6] Genzken.O, Brack.M. Temperature dependence of supershells in large sodium clusters. To be published and private communication.
- [7] Pederson.J, Bjørnholm.S, Borggreen.J, Hansen.K, Martin.T.P, Rasmussen.H.D. A new periodic system with three thousand elements. To be published, *Nature* (1991).
- [8] Martin.T.P, Bjørnholm.S, Borggreen.J, Bréchnignac.C, Cahuzac.Ph, Hansen.K, Pederson.J. Electronic shell structure of laser-warmed Na clusters. To be published, *Chem. Phys. Lett.* (1991).
- [9] Sattler.K, Mühlbach.J, Recknagel.E. Generation of metal clusters containing from 2 to 500 atoms. *Phys. Rev. Lett.* **45**, 821-824 (1980).
- [10] Franck.F, Schulze.W, Tesche.B, Urban.J, Winter.B. Formation of metal clusters and molecules by means of the gas aggregation technique and characterization of size distribution. *Surface Science* **156**, 90-99 (1985).
- [11] Bréchnignac.C, Cahuzac.ph, Carlier.F, de Frutos.M, Masson.A, Roux.J.Ph. Generation of rare earth metal clusters by means of the gas aggregation technique. *Z.Phys. D - Atoms, Molecules and clusters* **19**, 195-197 (1991).
- [12] Wiley.W.C, McLaren.I.H. Time-of-flight mass spectrometer with improved resolution. *The Review of Scient. Instrum.* **26**, 1150-1157 (1955).
- [13] Bréchnignac.C, Cahuzac.Ph, Carlier.F, Leygnier.J. Collective excitation in closed-shell potassium cluster ions. *Chem. Phys. Lett.* **164**, 433-437 (1989).
- [14] Bréchnignac.C, Cahuzac.Ph, Carlier.F, de Frutos.M, Leygnier.J. Cohesive energies of K_n $5 \leq n \leq 200$ from photoevaporation experiment. *J.Chem. Phys.* **93**, 7449-7456 (1990).
- [15] Knight.W.D, Clemenger.K, de Heer.W.A, Saunders.W.A, Chou.M.Y, Cohen.M.L. Electronic shell structure and abundances of sodium clusters. *Phys. Rev. Lett.* **52**, 2141-2143 (1984).
- [16] Bréchnignac.C, Cahuzac.Ph. Evolution of photoionization spectra of metal clusters as a function of size. *Z. Phys. D Atom, Molecules and clusters* **B**, 121-129 (1986).

- [17] Martin.T.P, Bergmann.T, Göhlich.H, Lange.T. Observation of electronic shells and shells of atoms in large Na clusters, *Chem. Phys.Lett.* **172**, 209-213 (1990).
 [18] Mansikka-aho.J, Suhonen.J, Valkealahti.S, Hammaren.E, Manninen.M.
 Electronic shell structure in icosahedral metal clusters, to be published (this issue).

STRUCTURE AND DYNAMICS OF INTERMEDIATE SIZE ALUMINIUM CLUSTERS

S. Debiaggi^{##} and A. Caro[#]

[#]Paul Scherrer Institute. 5232- Villigen. Switzerland.

^{*}Universidad Nacional del Comahue. 8300 Neuquen. Argentine.

ABSTRACT. We use molecular dynamics with a semiempirical quantum chemistry model at a Hartree level of approximation to predict the structure of Al_n clusters. The relative simplicity of this model allows us to relax up to few hundred atoms. We find that icosahedral and cuboctahedral symmetries are almost degenerate, but that for the cases where we performed annealing, deeper minima exist without symmetry.

1- Introduction:

Due to their simple electronic structure, Al clusters have been a favourite element in experimental and theoretical works. Compared to alkali metal clusters, they have the additional interest to s-p hybridize to form trivalent atoms becoming a bridge to transition metal clusters. The experimental data for Al cluster is very extensive; however, information on the cluster structures is still lacking and most of what is known comes from theoretical work. Density Functional - Simulated Annealing has been performed for Al_n [1], with n up to 10, leading to new stable structures (numerous buckled planar arrays are found), and spin multiplicities. Transitions from planar to non-planar structures are found at n = 5, and to states with minimum spin degeneracies at n = 6.

To our knowledge there is only one experimental report on dissociation energies of neutral clusters [2], which have been calculated through their measured dissociation energies for ionized clusters and the corresponding ionization potentials measured in photo-dissociation experiments. All calculations show poor agreement with these results. The SCF CI calculation of Petterson [3] and Upton [4] are substantially lower, while LSDA systematically overestimate the binding [1], (see Figure 1). For bigger Al clusters, ab-initio calculations are computationally very hard. For restricted geometries [5], and full annealed 13 and 55 atom clusters have been studied [6]. For Na [7] it has been found that low symmetry structures have less energy than their corresponding high-symmetry partners.

Semiempirical approaches become relevant as they can help in the search of global minima, extrapolate to regions of larger size, and enable predictions of the effects of temperature. Such type of results have been obtained by Pacchioni et al. [8] with an INDO method computed according to a symmetry restricted (no-relaxation of the structures) and spin unrestricted iterative procedure. Their calculation of cohesion extends up to n = 49, showing an overall trend as a function of cluster size which agrees with the experimental data, although still slightly lower than the measured values, (see Figure 1).

In this work we present results concerning Al clusters in the medium size region (n < 256). We use a simple quantum chemistry model, that properly describes the angular dependence of